

# FE analysis on the rate-dependent behaviour of model geosynthetic-reinforced soil retaining wall

Noguchi, T.

*CRC Solutions, 2-7-5 Minamisuna Koto-ku Tokyo, 136-8581, Japan*

Kongkitkul, W., Hirakawa, D. & Tatsuoka, F.

*Tokyo University of Science, 2641 Yamazaki Noda-shi Chiba, 278-8510, Japan*

Keywords: FEM, viscous, geosynthetics, time-dependency, bearing capacity

**ABSTRACT:** Not only geomaterial (i.e., clay, sand, gravel and soft rock) but also polymer geosynthetic reinforcement are known to exhibit more-or-less rate-dependent stress-strain or load-strain behaviour due to their viscous properties. Due to interactions between the elasto-viscoplastic properties of backfill and reinforcement, the rate-dependent deformation of backfill reinforced with polymer geosynthetic reinforcement becomes highly complicated. In the present study, incorporating elasto-viscoplasticity constitutive models of both sand and geogrid, plane strain FE analysis of the behaviour of a geosynthetic-reinforced soil retaining wall model vertically loaded with a rough rigid footing on the crest was performed.

## 1 INTRODUCTION

Geosynthetic-reinforced soil retaining walls (GRS-RW) exhibits more-or-less rate-dependent deformation due to the viscous properties of backfill and geosynthetic reinforcement. Interactions between the rate-dependent behaviours of soil and reinforcement make this issue very complicated. In the present study, plane strain elasto-viscoplastic FE analysis was performed incorporating non-linear three-component models of sand and polymer reinforcement to simulate results obtained from a loading test on a scaled-down GRS-RW model.

## 2 MODEL TEST

A scaled-down (i.e., 48 cm high) GRS-RW model with a full-height rigid facing was constructed in a sand box by tamping air-dried Toyoura sand in eight sub-layers to obtain a relative density equal to 90% (Figs. 1 and 2; Hirakawa, 2003). The backfill was reinforced with eight layers of a polyester geogrid. The model wall was vertically loaded via a 10 cm wide rigid rough footing placed on the crest of the backfill, allowing rotation about a line four cm above the footing base while without allowing translation of any moment. During otherwise monotonic loading, the vertical settlement rate of the footing was stepwise changed in a range between  $4.72 \times 10^{-3}$  and  $4.72 \times 10^{-1}$  mm/min and four stages of sustained loading were performed.

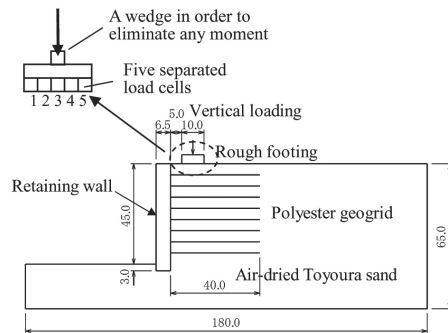


Figure 1. GRS-RW model (unit: cm).

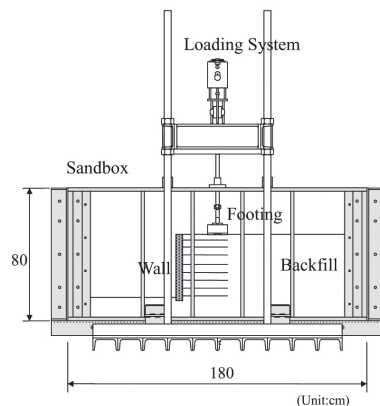


Figure 2. Test apparatus.

### 3 NON-LINEAR THREE-COMPONENT MODEL.

According to the non-linear three-component rheology model proposed by Di Benedetto et al. (2002) & Tatsuoka et al. (2002) (Fig. 3), a given strain increment is decomposed into elastic and irreversible components, while a given stress into inviscid and viscous components. They proposed a set of different models to simulate the effects of material viscosity on the stress-strain behaviour of different types of geomaterial (i.e., clay, sand, gravel and soft rock). It has been shown that the viscous property of saturated plastic clay can be characterised by the fact that the current stress during monotonic loading is a unique function of instantaneous irreversible strain and its rate (called the Isotach viscosity). On the other hand, the viscous property of clean sand (i.e., uniform sand) is different from the above in that the viscous effect decays with an increase in the irreversible strain, as described by a specific model called the TESRA model.

Hirakawa et al. (2003) applied the models to polymer reinforcements (i.e., polyester, Vinylon, HDPE, etc.) by replacing stress with tensile load. They showed that the viscous property of polyester reinforcement can be modelled by combining the Isotach and TESRA viscous properties, while the viscous property of the other polymer reinforcements examined is of the Isotach viscosity.

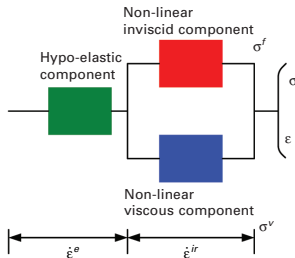


Figure 3. General non-linear three-component model proposed for geomaterial (Di Benedetto et al., 2002; Tatsuoka et al., 2002).

### 4 FEM SIMULATION OF LOAD-STRAIN RELATION OF GEOSYNTHETIC REINFORCEMENT

A biaxial type polyester geogrid having a centre-to-centre spacing of 18 mm in both longitudinal and transverse directions, coated with PVC resin for UV protection (Fig. 4) was used.

The FEM code developed by Siddiquee et al. (2003), which is able to realistically simulate the time-dependent behaviour of geosynthetic and geomaterial, was used in the present study. In order to simulate the reinforcement in FE analysis, the non-linear truss element was employed. Figure 5 shows

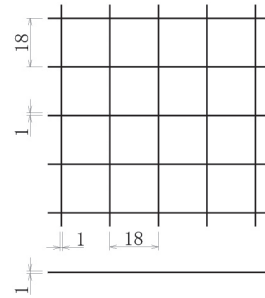


Figure 4. Configuration of polyester geogrid used in the model test described in this paper (unit: mm).

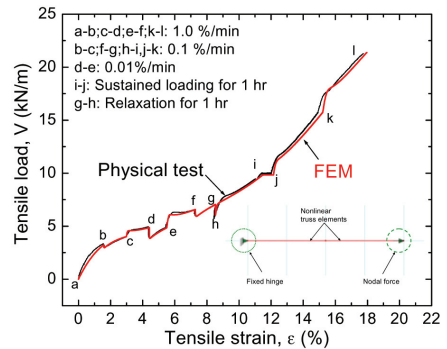


Figure 5. FE simulation of result from a tensile test on polyester grid.

the simulation of the result from a tensile test on the specimen described in Fig. 4 in which the strain rate was changed stepwise and sustained loading was performed during otherwise monotonic loading at a constant strain rate (Hirakawa et al., 2003). It may be seen that the proposed constitutive model can simulate rather accurately all the viscous aspects seen in the test result, including the creep behaviour.

### 5 FEM SIMULATION OF A MODEL GRS-RW

The backfill and the facing were modelled by four-node quadrilateral plane elements while the geogrid layers were modelled by truss elements (Fig. 6). The sand elements in contact with the respective geogrid layer were made weaker by a factor of 0.762 compared with the original value in the other part of the backfill. This adjustment is necessary to model the respective geogrid reinforcement layer having a covering ratio (CR) equal to 11.1% by a platen having CR = 100 % incorporated in the FE model (Peng et al., 2000). The TESRA viscous model parameters employed are:  $\alpha = 0.25$ ,  $m = 0.05$ ,  $(\dot{\epsilon}^{ir})_r = 10^{-8} \text{ s}^{-1}$  for the backfill; and  $\alpha = 0.55$ ,  $m = 0.12$ ,  $(\dot{\epsilon}^{ir})_r = 10^{-6} \text{ s}^{-1}$  for the geogrid. Vertical settlement vectors were given to the nodes at the footing base tracing the measured time history of footing settlement in the physical model test.

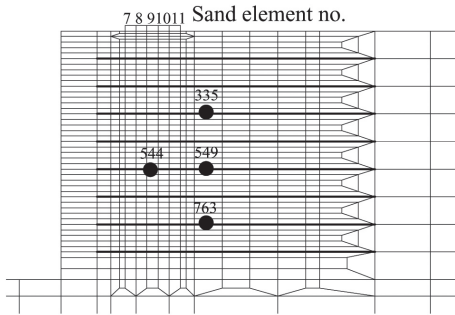


Figure 6. FE mesh for a model GRS-RW.

## 6 TEST RESULTS AND DISCUSSIONS

Figures 7, 8 and 9 show the  $q - s$  relation, the time history of  $q$ , and the time history of  $s$ , where  $q$  is the average footing pressure and  $s$  is the footing settlement.

Figure 7 compares the observed and simulated  $q - s$  relations. Cyclic loading stage, during which the behaviour is rather elastic, in the physical test was simulated by the sustained loading stage with the

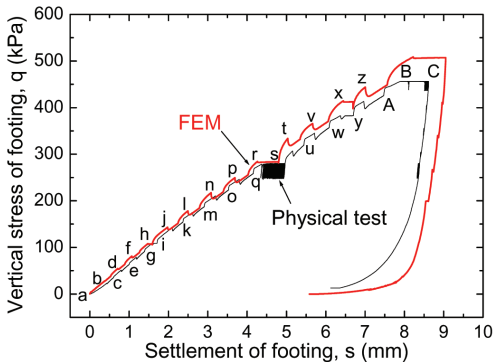


Figure 7. Observed and simulated footing pressure - settlement relations.

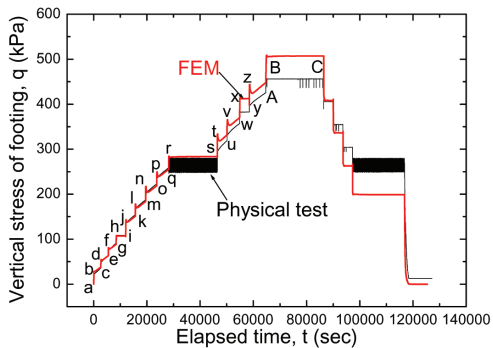


Figure 8. Observed and simulated time histories of footing pressure.

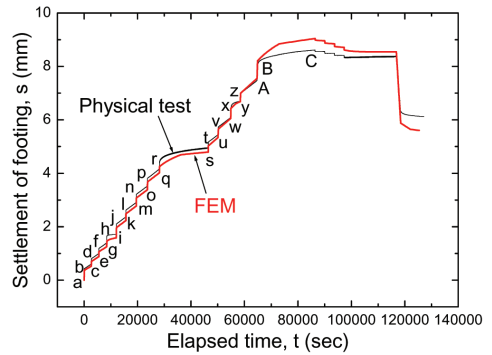


Figure 9. Observed and computed time histories of footing settlement.

equivalent time in the FE analysis. It may be seen that not only the overall measured  $q - s$  behaviour but also rate-dependent behaviour are well simulated. Fig. 10 shows deformation of the whole model at analysis step 1204 (i.e., stage B in Fig. 8). Fig. 11 compares the observed and simulated time histories of local footing base pressure. The footing base was equipped with five load cells. Load cell Nos. 1 and 5 are located at the footing toe, close to the facing, and the footing centre. The trend of jump in local vertical stress upon stepwise changes in settlement rate is well simulated. However, the local vertical stress value at Load cell No. 1 is largely over-predicted while the opposite is true with Load cell No. 5, in contrast to a satisfactory simulation of the overall  $q - s$  behaviour (Figs. 7, 8 & 9).

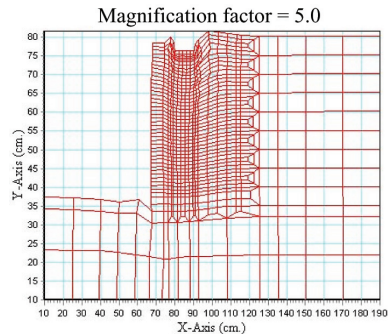


Figure 10. Computed deformation of the model wall.

Figure 12 compares the measured and simulated time histories of local tensile strain developed at the locations in the geogrid depicted in Fig. 6. The overall time histories of tensile strain of geogrid are generally well simulated by FEM. However, the details of the rate-dependency of the local-strain behaviour of geogrid are not very satisfactorily simulated. Therefore, further study will be necessary in this respect.

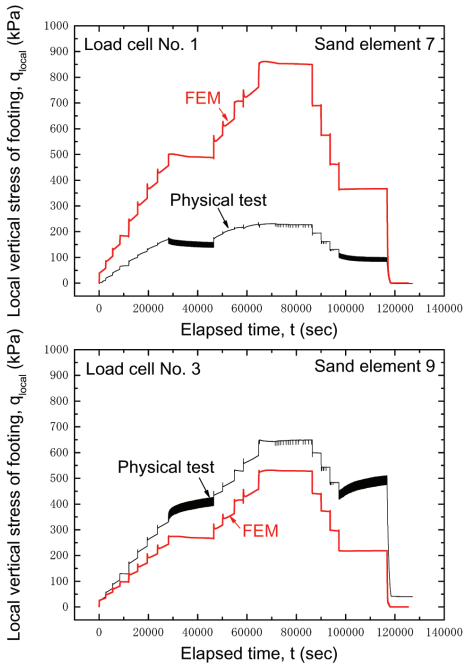


Figure 11. Observed and simulated time histories of local vertical footing pressure at load cell Nos. 1 & 3.

## 7 CONCLUSIONS

1. Only by incorporating the elasto-viscoplastic properties of both backfill (i.e., sand) and polymer geogrid reinforcement, FE analysis can realistically simulate the rate-dependent behaviour of geogrid-reinforced soil retaining wall. The viscous properties of sand and polyester reinforcement can be modelled by the non-linear three-component model described in this paper.
2. Despite that the analysis was not totally satisfactory, the rate-dependent behaviour, including creep deformation, of a physical model wall vertically loaded with a rough rigid footing placed on the crest of the backfill was simulated rather well by plane strain FE analysis.

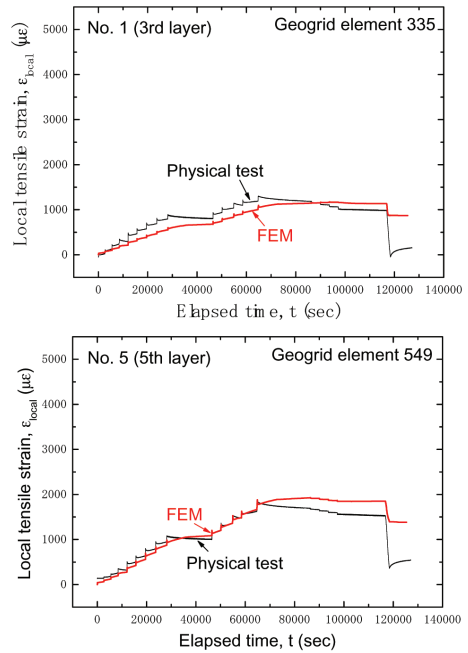


Figure 12. FE simulation of time histories of local tensile strain in the geogrid.

## REFERENCES

- Di Benedetto, H., Tatsuoka, F. and Ishihara, M. (2002). "Time-dependent shear deformation characteristics of sand and their constitutive modelling", *Soils and Foundations*, Vol. 42 (2), pp. 1-22.
- Hirakawa, D. (2003). "Study on residual deformation characteristics of geosynthetic-reinforced soil structures", *Ph.D. Thesis*, University of Tokyo (in Japanese).
- Hirakawa, D., Kongkitkul, W., Tatsuoka, F. and Uchimura, T. (2003). "Time-dependent stress-strain behaviour due to viscous properties of geosynthetic reinforcement", *Geosynthetics International*, Vol. 10 (6), pp. 176-199.
- Peng, F.L., Kotake, N., Tatsuoka, F., Hirakawa, D. and Tanaka, T. (2000). "Plane strain compression behaviour of geogrid-reinforced sand and its numerical analysis", *Soils and Foundations*, Vol. 40 (3), pp. 55-74.
- Tatsuoka, F., Ishihara, M., Di Benedetto, H. and Kuwano, R. (2002). "Time-dependent shear deformation characteristics of geomaterials and their simulation", *Soils and Foundations*, Vol. 42 (2), pp. 103-138.